Decadal and Long-term Variability of Sea Level in the Southwestern Pacific during 1948-2018

Jingxuan Sun[1,2,3], Linlin Zhang[1,2,3,4], Dunxin Hu[1,2,4]

[1] Key Laboratory of Ocean Circulation and Waves, Institute of Oceanology, Chinese Academy of Sciences, Qingdao 266071, China

[2] Pilot National Laboratory for Marine Science and Technology (Qingdao), Qingdao 266237, China

[3] University of Chinese Academy of Sciences, Beijing 100049, China

[4] Center for Ocean Mega-Science, Chinese Academy of Sciences, Qingdao 266071, China

Corresponding author: Linlin Zhang (zhanglinlin@qdio.ac.cn)

Key Points:

- 70-year-long tide gauge records near New Zealand exhibit an increasing trend in sea level accompanied by pronounced decadal oscillations
- WSC anomalies associated with SAM and IPO modulate the SWP sea level variability on long-term and decadal time scales
- Long-term sea level trend is due to local wind forcing, while decadal oscillations are dominated by both local and remote factors

Abstract

Decadal and Long-term variability of sea level in the Southwestern Pacific (SWP) is investigated with tide gauge measurements near New Zealand ranging from 1948 to 2018 and a 1.5-layer reduced gravity model. After removing the global mean sea level, SWP sea level still exhibits a prominent increasing trend accompanied by strong decadal oscillations, which is attributed to the Southern Annular Mode (SAM) and Interdecadal Pacific Oscillation (IPO), respectively. On the long-term time scale, the intensification of local wind stress curl associated with strengthening SAM contributes to the SWP sea level rise through Ekman convergence. On the decadal time scale, locally generated and westward propagating signals induced by IPO exert comparable influences on the sea level variations in the SWP. Multi-variable linear regression analysis suggests that SAM and IPO account for approximately 83% and 58% of the tide gauge sea level variability on long-term and decadal time scales, respectively.

Plain Language Summary

Satellite altimeter observations show a prominent acceleration in sea level rise in the western Pacific during 1993-2018, which has crucial implications for the economic development and livelihoods in coastal countries. Regional sea level variations associated with basin-scale climate modes differ significantly from the global average on both temporal and spatial scales. Extensive studies have shown that the above apparent sea level rise in the western tropical Pacific

during altimeter era is essentially a decadal signal after removing the global mean sea level, which are generally considered to be generated by direct wind stress forcing in connection with IPO. Based on long-term tide gauge records near New Zealand, this work highlights the influence of different climate modes on the low-frequency variability of sea level in the SWP, and their differences from the tropics in terms of characteristics and mechanisms. After removing the global mean sea level, there still exists a persistent upward trend in sea level accompanied by a pronounced decadal oscillation, which is found to be associated with SAM and IPO. Physically, anomalous wind stress curl related to climate modes modulates sea level variability in the SWP via both local Ekman pumping and remote baroclinic Rossby waves.

1 Introduction

Global mean sea level (GMSL) has been rising rapidly at a rate of about 0.15 cm/year since the early 20th century (Frederikse et al., 2020) and is predicted to continue rising in the coming decades (Fasullo & Nerem, 2018). This is related to alterations in ocean dynamics and land-ice input under a global warming background (e.g., Cazenave et al., 2019; Dangendorf et al., 2019). Nevertheless, this rising signal has a significant spatial pattern and is not globally consistent (e.g., Church et al., 2011; Chen et al., 2019). Particularly, during the past 2-3 decades of the altimetry era, sea level in the western Pacific exhibits the most arresting rising trend across the global ocean, and the rate is around 0.6 cm/year, almost twice higher than the global average during the same period (Figure 1a; e.g., Church et al., 2004; Nerem et al., 2010; Qu et al., 2019). The potential impact of sea level rise on modern coastal residents and society has brought this issue to urgent attention in this region (Merrifield et al., 2011).

The prominent regional sea level rising in the western Pacific is partly attributed to the GMSL rising (e.g., Nerem et al., 2010; Merrifield et al., 2012; Chen et al., 2017). However, after subtracting the GMSL, sea level in the western Pacific, including both the tropical and subtropical, still shows a significant rising trend (Figure 1b). The low-frequency variations of sea level in the western tropical Pacific (WTP) since the 1950s have been extensively studied based on tide gauge measurements, reconstructed products and numerical simulations (e.g., Feng et al., 2004; Becker et al., 2012; Merrifield et al., 2018). The accelerating sea level rising in the WTP over the last 2-3 decades after removing the GMSL is revealed to be driven by the wind stress forcing associated with IPO (e.g., Merrifield et al., 2012; Hamlington et al., 2013).

In comparison, the sea level variability in the SWP and its relationship with climate modes remain inconclusive yet. Cai (2006) and Roemmich et al. (2007) indicate that the subtropical gyre spin-up and associated sea level rise over the South Pacific in the past decades are tightly linked to SAM. Sasaki et al. (2008) investigates the low-frequency variability of sea level anomaly (SLA) east of New Zealand during 1970-2003 based on model outputs, and reports significant decadal variations of the sea level, which is further attributed to wind stress curl (WSC) anomalies associated with the decadal modulation of El

Niño–Southern Oscillation (ENSO). The de-trended sea level time series from Fort Denison tide gauge station located in the Sydney Harbor also presents apparent decadal variations highly related to PDO (Holbrook et al., 2011). In addition, anthropogenic forcing seems to contribute to the sea level rise over the South Pacific in recent decades as well (Albrecht et al., 2019). Actually, the low-frequency component of both SAM and IPO are exhibited as trends during the altimetry era, and potentially induce the rapid sea level rising in the SWP through WSC forcing. However, due to the short duration of satellite observations and the limited reliability of model simulations, few prior studies have separated the contributions from these two climate modes despite of their importance in understanding and predicting the sea level variations in the South Pacific.

In this study, we investigate the long-term and decadal variability of sea level based on tide gauge data off New Zealand. The 70-year-long records enables us to distinguish between the effects of SAM and IPO on sea level variations in the SWP. An increasing trend of sea level with strong decadal variations is detected from the tide gauge records even after removing the GMSL (Figure 1d), which are regulated by WSC forcing associated with SAM and IPO, respectively. Further, we perform a quantitative estimation on the relative contributions of local and remote wind forcing to the low-frequency sea level variability using a 1.5-layer reduced gravity model (RGM).

2 Data and Methods

2.1 Data

Monthly sea level time series downloaded from the Permanent Service for Mean Sea Level (PSMSL; Woodworth et al., 2003) at two tide gauge stations in the western Pacific are used. To eliminate the interannual fluctuations, a 7-year running mean is performed in advance. These two stations are Wellington station located at 41.28°S, 174.78°E and Appa Harbor station at 13.44°N, 144.65°E (Figure 1b). The observation period of the two time series spans from 1948 to 2018. The weekly SLA data with a resolution of $0.25° \times 0.25°$ on Mercator grid provided by Archiving Validation, and Interpretation of Satellite Oceanography (AVISO; Le Traon et al., 1998) for the period from January 1993 to December 2018 is also used. We calculate the relative trends of sea level from PSMSL and AVISO products during their overlapping period to evaluate the trends from the vertical land motion. The difference between these two trends is considered constant over the entire recording time range of each tide gauge (Nerem & Mitchum, 2002). In addition, the Institute of Atmospheric Physics (IAP) gridded steric sea level (SSL) reconstruction from 1948-2018 are utilized for comparison (Cheng et al., 2017). Monthly wind stress data on the T62 Gaussian horizontal grid during 1948-2018 are obtained from the National Centers for Environmental Prediction–National Center for Atmospheric Research (NCEP–NCAR) reanalysis (Kalnay et al., 1996), and used to drive the RGM.

2.2 1.5-layer reduced gravity model

To gain more insight into the mechanism of sea level variability, we conduct a series of experiments with the RGM. This model has been extensively employed in previous studies to investigate the sea level variability caused by baroclinic response of the ocean to WSC forcing (e.g., Fu & Qiu, 2002; Schneider et al., 2002). We examine whether wind-driven long Rossby waves can account for the decadal to long-term sea level variations recorded by tide gauges in the SWP, and then the contributions of wind forcing from different regions are quantitatively analyzed through wind shielding experiments. These experiments are necessary for a clear understanding of the sea level variability on multiple time scales. The RGM explaining the dynamics restrained by the linear vorticity equation under a long-wave approximation is the same as Qiu and Chen (2006), and the contribution from SLA signals along the eastern boundary is ignored, which has little effect on the western basin.

2.3 Nonlinear trend estimation method

An adaptive data analysis method of the ensemble empirical mode decomposition (EEMD) is used here to extract the nonlinear trends (Huang & Wu, 2008). As an upgraded version of the empirical mode decomposition (EMD) method (Huang et al., 1998), EEMD has been applied in many geophysical investigations to process the nonlinear data and obtain their trends (e.g., Wu & Huang, 2009; Qian, 2015). The last component of the EEMD results (hereafter R_n (t)) is treated as the nonlinear trend. To facilitate the comparison of the EEMD trend with the corresponding linear trend, the EEMD trend is further calculated as $\mathrm{Trend_{EEMD}}$ = [R_n (end) - R_n (start)] / (length (Rn)), similar to Ji et al. (2014).

3 Results

3.1 Sea level variations

Figure 1a shows the linear trend of sea level in the global ocean during 1993-2018 derived from satellite altimetry. It is obvious that the western Pacific is featured with prominent regional sea level rise, reflecting the moderating effects of climate modes as suggested by Han et al. (2019). Two significant sea level rising signal is observed in the western Pacific, with one locating in the WTP and another appearing east of New Zealand in the SWP. Even after removal of the rising GMSL, obvious increasing trend still exists in the two regions (Figure 1b). These characteristics are consistent with previous studies based on satellite altimetry, tide gauge measurements and model simulations (e.g., Sasaki et al., 2008; Nerem et al., 2010).

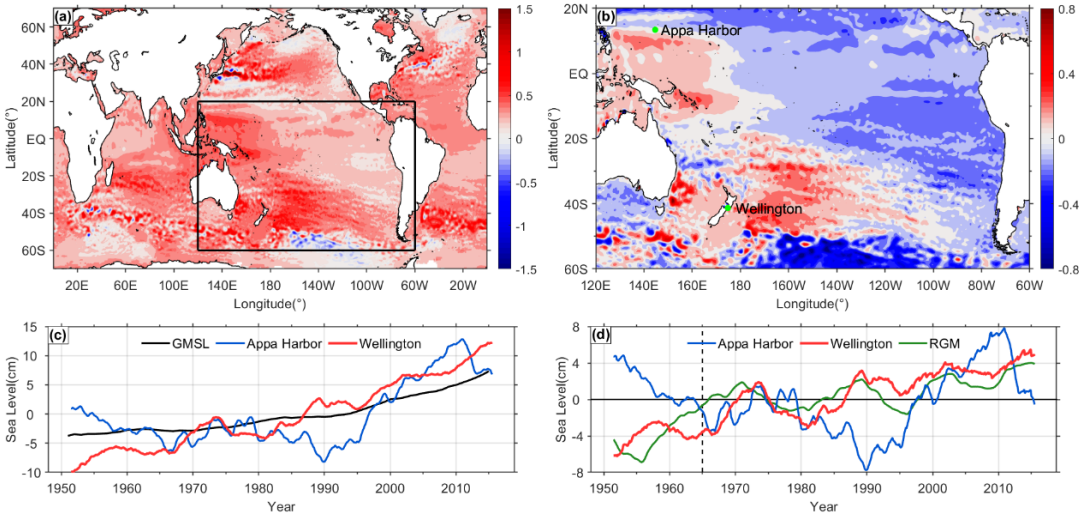

Figure 1. (a) Linear trend (cm/yr) of SLA during 1993-2018 from the AVISO multi-mission gridded product. (b) Same as (a) but for the South Pacific, with the GMSL being removed. Green dots indicate Wellington (41.28°S, 174.78°E) and Appa Harbor (13.44°N, 144.65°E) tide gauge stations. (c) SLA time series (cm) at Wellington (red) and Appa Harbor (blue) during 1948-2018 from PSMSL. Black curve shows the GMSL time series. (d) Same as (c), but the GMSL has been subtracted. The green curve is for RGM-simulated SLA time series near New Zealand (41°S, 176°E). All the time series during 1948-2018 have been smoothed with a 7-year low-pass filter.

The two pronounced sea level rising signals in the western Pacific during the altimeter era is also revealed by tide gauge records (Figure 1c). Longer time series from tide gauges in the WTP over the past 70 years suggests that the low-frequency sea level variations are composed of a long-term trend due to the GMSL rising and a decadal oscillation associated with IPO, which has been reported by Merrifield et al. (2012). Here, Appa Harbor station, a very regionally representative station in this region, is selected to reproduce the results (Figure 1c-1d, in comparison with Figure 2 in Merrifield et al. [2012]). Obviously, it is the superposition of the long-term trend and decadal oscillation that produces the rapidly rising trend of sea level during the altimetry era. While the situation seems different at Wellington station, the only continuously operating station near New Zealand in the SWP with long-term records, at least back to the 1950s. After removing the GMSL, the tide gauge records still demonstrate an increasing trend of 0.14 cm/year accompanied by noticeable decadal variations (Figure 1d).

To investigate the sea level variations across the Pacific basin rather than that just near the New Zealand coast, the gridded SSL reconstruction from IAP is analyzed. SSL anomalies along 41°S in the Pacific with a 7-year low-pass filter are shown in Figure 2a. Here, the steric-GMSL has been removed so that the

SSL anomaly time series is comparable with the tide gauge records in Figure 1d. The results indicate that the sea level rising signals and the decadal modulations appear almost in the entire longitude range of the South Pacific basin, and westward propagating signals could be seen, especially after 1980. For example, a negative sea level signal originates in the eastern Pacific around 1980, and it takes about 10 years to reach the western boundary. Such propagating signals are insignificant before 1980, which is probably due to the sparse observations in the early decades. Large-scale interpolating and smoothing used in the SSL reconstruction may bring non-ignorable bias during the early years.

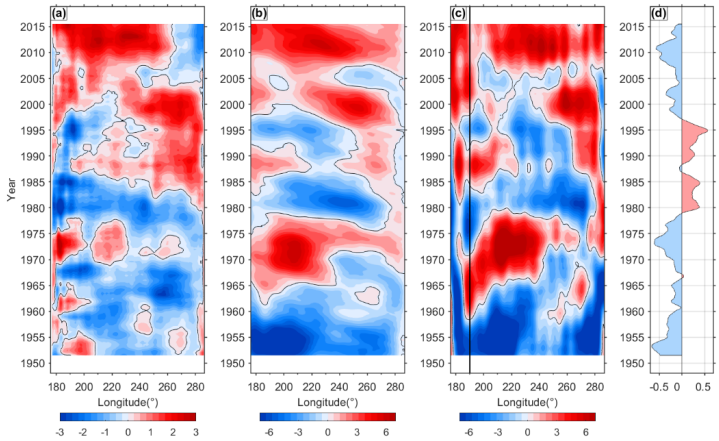

Figure 2. (a) Hovmöller diagram of SSL anomalies (cm) along 41°S from IAP dataset. (b) and (c) are similar to (a), but for the sea level anomalies derived from RGM and Ekman pumping dynamics, respectively. Black line in (c) indicates 170°W. (d) Normalized IPO index. All the time series are during 1948-2018 and have been smoothed with a 7-year low-pass filter.

3.2 Dynamics of sea level variability

The decadal variability of sea level in the South Pacific is suggested to be driven by basin-scale WSC anomalies in previous studies (e.g., Qiu & Chen, 2006; Zhang & Qu, 2015; Han et al., 2019). SLA signals induced by WSC variations in the central-eastern Pacific propagate westward in the form of baroclinic Rossby waves and then modulate sea level pattern in the western Pacific. Here, we employ a 1.5-layer RGM to simulate this process. The Newtonian dissipation rate and reduced gravity are 0.3 and 0.06 m/s^2, respectively. The RGM is forced by monthly WSC anomalies derived from NCEP–NCAR 10m-wind from 1948 to 2018, and the model results are compared with the sea level time series from the tide gauge (Figure 1d). Based on the first mode baroclinic Rossby wave speed derived by Chelton et al. (1998) with a latitude-dependent amplification factor, it takes about 10-15 years for SLA signals at the eastern boundary to cross the entire basin at the latitude analyzed in this study. Thus, in the following analysis, we use the model results after 1965 when the model has been integrated for more than 15 years. The long-term increasing trend of sea level accompanied

by decadal variations at Wellington station is well captured by the RGM, and the correlation between the model simulation and tide gauge records reaches 0.6 (Figure 1d). The Hovmöller diagram of modeled sea level anomalies is also compared with the IAP reconstruction (Figure 2a-2b), and they are generally consistent with each other. Above consistency implies that the decadal and long-term variations of sea level in the SWP are primarily regulated by the WSC variability via baroclinic Rossby wave adjustment process.

3.2.1 Long-term trend

It is known that SAM serves as the most important climate mode in the Southern Hemisphere, which has experienced a pronounced upward trend during the past several decades (Thompson et al., 2000). The SAM index is derived here by calculating a normalized difference of monthly zonal mean sea level pressure between 40°S and 65°S following Stocker et al. (2013), and then WSC anomaly fields during 1948-2018 over the South Pacific are regressed linearly onto the SAM index (Figure 3a). A 7-year low-pass filter is used before the regression to eliminate interannual fluctuations. Positive WSC anomalies occupy almost the entire Pacific basin south of 40°S, with a strong anomaly patch appearing east and south of New Zealand. The convergence induced by the WSC anomalies could potentially explain the sea level rising recorded by the tide gauge at Wellington.

Sea level variability could be governed by both local Ekman pumping and remote baroclinic Rossby wave dynamics. To quantify the relative contributions of different factors on the long-term sea level rising, three experiments are conducted with the RGM. The control (CTL) run is forced by NCEP-NCAR WSC anomalies along 41°S, which includes both local and remote wind forcing across the South Pacific basin. Experiment 1 (EXP1) and experiment 2 (EXP2) are the same as the CTL run, but the WSC anomalies east and west of 170°W are set to be zero, respectively. Therefore, EXP1 and EXP2 correspond to the local forcing run and remote forcing run. In EXP1, the local wind forcing simulates a conspicuous upward trend of sea level with a slope of 0.79 cm/decade, slightly faster than the CTL run (Figure 3b). In EXP2, the remote wind field in the central-eastern Pacific mainly produces decadal sea level signals near New Zealand and even induces a weak decreasing trend of -0.15 cm/decade (Figure 3b). In hence, the sea level rising in the SWP is primarily due to the local WSC forcing on the long-term time scale.

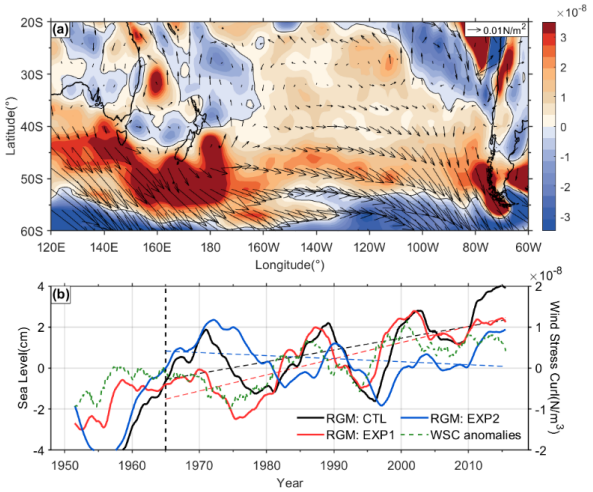

Figure 3. (a) Linear regression of NCEP–NCAR 10m-wind stress (vectors; N/m^2) and WSC anomalies (color; N/m^3) in the South Pacific onto the normalized SAM index. (b) Sea level anomalies (cm) near New Zealand simulated by the RGM CTL run (black), EXP1 (red), and EXP2 (blue). The corresponding dashed lines indicate the linear trends. Green dashed curve represents the regional mean WSC anomalies (N/m^3) along 41°S west of 170°W. All the time series are during 1948-2018 and have been smoothed with a 7-year low-pass filter.

As the dominant climate mode in the Southern Hemisphere, SAM has been strengthening during the recent decades, which is accompanied by the intensification of mid-latitude westerly winds (e.g., Thompson et al., 2000; Cai, 2006). The enhanced Ekman convergence due to positive WSC anomalies in the northern flank of the westerly wind near New Zealand leads to the accumulation of water mass and the rise of sea level. We also check the regional mean of local WSC anomalies and find a good agreement with the results of EXP1 (Figure 3b), confirming that the long-term component of local wind associated with SAM plays a dominant role in the persistent trend of sea level rising near New Zealand since the 1950s.

It should be noted that the decreasing trend simulated by EXP2 does not contradict the positive WSC anomalies over the whole South Pacific basin in the regression results (Figure 3a). The WSC pattern is the simultaneous regression of the SAM index and WSC anomaly fields, while the modeled results of EXP2 reflect the integration process of westward propagating Rossby waves across the Pacific basin over 10-15 years.

3.2.2 Decadal variability

On the decadal time scale, the most significant oscillation in the Pacific is IPO, which is accompanied by pronounced wind forcing modulations (Henley et al.,

2015). The decadal component of sea level variations recorded by the tide gauge near New Zealand shows a negative correlation with IPO index (Figure 4b). Similar to Figure 3a, but for the IPO index ranging from 1948 to 2018, the regression pattern of WSC anomalies is obtained (Figure 4a). In fact, the most prominent signature of IPO appears in the equatorial Pacific, where trade wind stress forcing strongly modulates the sea level variations on the multidecadal time scale, which has been investigated by previous studies based on long-term tide gauge records in the WTP (Merrifield et al., 2012). In the SWP, especially in the latitude band of 30°-50°S, there exist a negative WSC anomaly pattern in the central-eastern basin, and a positive pattern east of New Zealand (Figure 4a).

To distinguish the effects of local and remote WSC forcing associated with IPO on the decadal sea level variations near New Zealand, we obtain decadal components of the model results from the CTL run, EXP1, and EXP2 (hereafter dCTL, dEXP1, dEXP2) by subtracting their long-term trends (Figure 4b-4c). The high correlation between dCTL and the decadal component of tide gauge records at Wellington station suggests that the decadal signal is simulated well by the RGM control run (Figure 4b). The STD of dCTL, dEXP1, and dEXP2 are 1.18 cm, 0.97 cm, and 0.94 cm, respectively, which indicates the process of local and remote wind forcing are both indispensable for the decadal variability here.

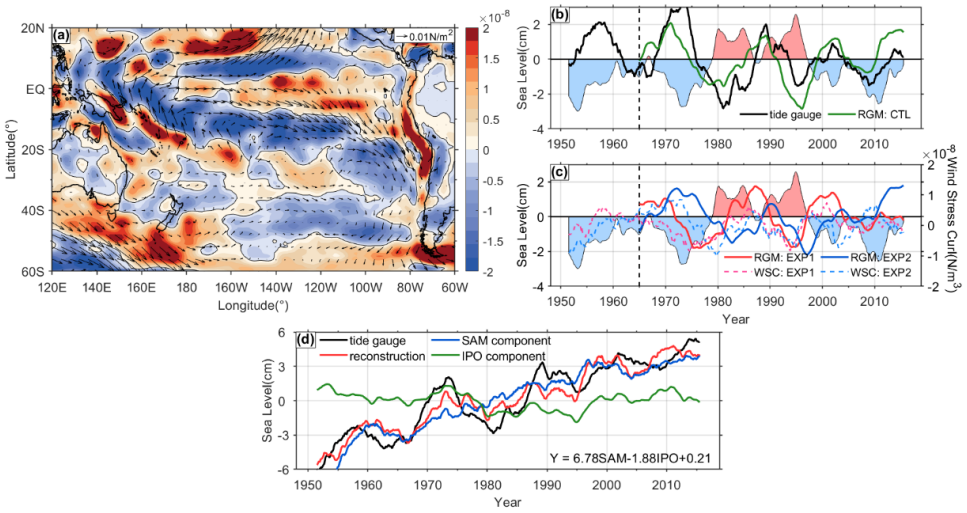

Figure 4. (a) Linear regression of NCEP–NCAR 10m-wind stress (vectors; N/m^2) and WSC anomalies (color; N/m^3) in the South Pacific onto the normalized IPO index. (b) Decadal components of sea level anomalies (cm) from tide gauge records at Wellington station (black) and RGM CTL run (green). (c) Same as (b), but for EXP1 (red solid) and EXP2 (blue solid) simulations. The corresponding dashed lines indicate decadal variations of regional mean WSC anomalies (N/m^3) along 41°S west (red) and east (blue) of 170°W. Bars in (b)

and (c) represent the 4.5 times normalized IPO index. (d) Tide gauge records at Wellington (black) and regressed SLA (red) with normalized SAM and IPO index. Blue and green curves indicate SAM and IPO component, respectively. All the time series are during 1948-2018 and have been smoothed with a 7-year low-pass filter.

Furtherly, the Hovmöller diagram of CTL run-simulated sea level anomalies along 41°S after a 7-year low-pass filter is presented to explore the oceanic response to wind forcing (Figure 2b). Take the decadal events during 1980-1995 as an example, when the IPO is in positive phase, negative WSC anomalies appear in the central-eastern Pacific, and the associated Ekman divergence induces negative SLA signals immediately. Although accompanied by dissipation and attenuation, those negative SLA signals still propagate westward as baroclinic Rossby waves and reach the western boundary partly. The time-lag relationship between dEXP2 and the decadal component of regional mean WSC anomalies east of 170°W reflects the propagating process of baroclinic Rossby wave as well (Figure 4c).

However, the regression pattern shows positive WSC anomalies near the New Zealand coast during the positive phase of IPO (Figure 4a), which raise the sea level through local Ekman convergence. It seems contrary with the phenomenon that the sea level records are negatively correlated with IPO (Figure 4b). To investigate this disagreement, we examine the Hovmöller diagram of sea level anomalies induced by Ekman pumping along 41°S (Figure 2c). In fact, although the simultaneous regression displays positive WSC anomalies, the fingerprints of IPO in local wind field and associated sea level anomalies are dynamic. When the IPO index reverses sign, local regions will response with delayed sea level anomalies after 3-5 years. The decadal variation of regional mean WSC anomalies west of 170°W also presents a lagged, in-phase response to IPO mode after several years, which results in the delayed sea level variations (Figure 4c).

Generally speaking, the fingerprint of IPO in the wind filed is composed of WSC anomalies in both local and interior ocean. These two WSC anomalies modulate the sea level variability near New Zealand together on the decadal time scale through local Ekman pumping and remote baroclinic Rossby wave propagation. In addition, it should be mentioned that the time series simulated by the RGM and recorded by the tide gauge are not exactly comparable, since the former only reflects the wind-driven component while the latter also includes the water mass component. Nevertheless, the effect of water mass on the sea level variability in the local region of the SWP studied here is little according to recent studies (Chen et al., 2019), therefore we neglect the water mass effect in this study.

3.2.3 Contribution of climate modes

According to the above analysis, SAM and IPO have contributed to the sea level rise in the SWP through WSC forcing over the past several decades. However, due to the lack of long-term observations, the effects of these two climate modes on the sea level variability have not been distinguished before, despite their

significance in promoting the comprehension of sea level and associated ocean circulation changes in the South Pacific (e.g., Cai, 2006; Roemmich et al., 2007; Sasaki et al., 2008; Zhang & Qu, 2015; Dangendorf et al., 2021).

Here, to quantify the influence of SAM and IPO, a multi-variable linear regression analysis is performed between the tide gauge records and these two indices (Figure 4d). It could be seen that the reconstructed time series with these two climate indices well reproduces the decadal and trend signals (Figure 4d). The regression equation can be expressed as Y = 6.78SAM - 1.88IPO + 0.21, where Y represents the reconstructed results. SAM and IPO have been normalized before the regression. Then, we obtain the decadal and long-term reconstructed components that are associated with SAM and IPO to estimate the contribution of the two climate modes to sea level variations (Figure 4d). The EEMD trend rates of the tide gauge records and the SAM component are 0.17 cm/year and 0.14 cm/year, respectively. Thus, SAM explains about 83% of the long-term sea level variations. After extracting their EEMD trends, the decadal variation of the tide gauge records and the IPO component is compared, and their STD are 1.31 cm and 0.76 cm, implying that IPO accounts for about 58% of the decadal variation of the sea level.

4 Summary and Discussion

Sea level rise and its ecological and social impacts, especially in low-lying coastal areas and island nations, have attracted widespread attention under the global climate change (e.g., Fasullo et al., 2018; Frederikse et al., 2020). Coastal sea level variability is mainly modulated by wind forcing associated with basin-scale climate modes (Han et al., 2019). However, due to the lack of long-term observational data, few previous studies has separated the effects of major climate modes on sea level rise in the SWP, one of the most prominent rising regions in the global ocean. Based on a 70-year-long tide gauge records near the New Zealand coast, the long-term and decadal variability of sea level during 1940-2018 are investigated. The sea level exhibits a clear upward trend accompanied by strong decadal variations even after removing the GMSL, which can be reasonably explained by the WSC forcing associated with SAM and IPO, respectively. It is different from that in the WTP where the sea level is basically regulated by PDO through wind stress forcing (Merrifield et al., 2012). Furtherly, multi-variable linear regression indicates that SAM explains 83% of sea level rise on the long-term time scale, while IPO accounts for about 58% of decadal variations. Reduced gravity model experiments suggest that both dynamic processes of remote baroclinic Rossby wave propagation and local Ekman pumping are essential to the decadal variability of sea level in the SWP, while local Ekman pumping dominates the long-term sea level trend.

It is worth noting that this work is concentrated on the wind-driven dynamic sea level, reflecting the undulation of isopycnals. The property variations of water mass are not captured by the reduced gravity model. Besides, the impact of freshwater imports is ignored as well, which is considered as an insignificant factor on sea level variability in the SWP (Chen et al., 2019). To achieve

a profound understanding of the sea level variability, more efforts should be devoted to distinguishing relative contributions of above factors.

In addition, the results reported here focus on the local sea level variations in the SWP. Considering that IPO and SAM are basin-scale modes, we investigate the low-frequency sea level variations in the whole South Pacific based on IAP dataset. Preliminary results show that the dominant signal is still an upward trend associated with SAM after removing the GMSL. But the decadal sea level variation and its relationship with the synchronous regulating processes of AMO, IPO, and other climate modes still remain unclear (e.g., Chen et al., 2019; Duan et al., 2021). Further exploration with more observations or numerical experiments is necessary in future studies.

Acknowledgement

The authors are grateful to Dr. Tangdong Qu for useful discussion on this topic. This study is supported by the National Natural Science Foundation of China (No. 41776021 and 42122041), National Key Research and Development Program of China (No. 2020YFA0608801). Tide gauge data is provided by the Permanent Service for Mean Sea Level (www.psmsl.org). Satellite altimetry data is downloaded from https://resources.marine.copernicus.eu/product-download/SEALEVEL_GLO_PHY_L4_REP_OBSERVATIONS_008_047. IAP dataset is obtained from http://www.ocean.iap.ac.cn/pages/dataService/dataService.html?languageType=en& NCEP reanalysis products are available at http://www.psl.noaa.gov/data/gridded/data.ncep.reanalysis.derived IPO index can be found at https://psl.noaa.gov/data/climateindices/list/.

References

Albrecht, F., Pizarro, O., Montecinos, A., & Zhang, X. (2019), Understanding sea level change in the South Pacific during the late 20th century and early 21st century. *Journal of Geophysical Research: Oceans, 124*, 3849–3858. doi: 10.1029/2018JC014828

Becker, M., Meyssignac, B., Letetrel, C., Llovel, W., Cazenave, A., & Delcroix, T. (2012), Sea level variations at tropical Pacific islands since 1950. *Global and Planetary Change, 80-81*, 85-98. doi: 10.1016/j.gloplacha.2011.09.004

Bromirski, P. D., Miller, A. J., Flick, R. E., & Auad, G. (2011), Dynamical suppression of sea level rise along the Pacific coast of North America: Indications for imminent acceleration. J*ournal of Geophysical Research: Oceans, 116*, C07005. doi: 10.1029/2010JC006759

Cai, W. (2006), Antarctic ozone depletion causes an intensification of the Southern Ocean super-gyre circulation. *Geophysical Research Letters, 33*, L03712. doi: 10.1029/2005GL024911

Cazenave, A., Hamlington, B., Horwath, M., Barletta, V. R., Benveniste, J., Chambers, D., et al. (2019), Observational requirements for long-term monitoring of the global mean sea level and its components over the altimetry era. *Frontiers in Marine Science, 6*, 582. doi: 10.3389/fmars.2019.00582

Chelton, D. B., Deszoeke, R. A., Schlax, M. G., El Naggar, K., & Siwertz, N. (1998), Geographical variability of the first baroclinic Rossby radius of deformation. *Journal of Physical Oceanography, 28*(3), 433-460. doi: 10.1175/1520-0485(1998)028<0433:GVOTFB>2.0.CO;2

Chen, C., Liu, W., & Wang, G. (2019), Understanding the uncertainty in the 21st century dynamic sea level projections: The role of the AMOC. *Geophysical Research Letters, 46*, 210–217. doi: 10.1029/2018GL080676

Chen, X., Zhang, X., Church, J.A., Watson, C.S., King, M.A., Monselesan, D., et al. (2017), The increasing rate of global mean sea-level rise during 1993-2014. *Nature Climate Change, 7*, 492-495. doi:10.1038/NCLIMATE3325

Cheng, L., Trenberth, K. E., Fasullo, J., Boyer, T., Abraham, J., & Zhu, J. (2017), Improved estimates of ocean heat content from 1960 to 2015. *Sci. Adv, 3*, e1601545. doi: 10.1126/sciadv.1601545

Church, J.A., Gregory, J.M., White, N.J., Platten, S.M., & Mitrovica, J.X. (2011), Understanding and projecting sea level change. *Oceanography 24*(2), 130–143. doi: 10.5670/oceanog.2011.33

Church, J. A., White, N. J., Coleman, R., Lambeck, K., & Mitrovica, J. X. (2004), Estimates of the regional distribution of sea level rise over the 1950–2000 period. *Journal of Climate, 17*(13), 2609-2625. doi: 10.1175/1520-0442(2004)017<2609:EOTRDO>2.0.CO;2

Dangendorf, S., Frederikse, T., Chafik, L., Klinck, J. M., Ezer, T., & Hamlington, B. D. (2021), Data-driven reconstruction reveals large-scale ocean circulation control on coastal sea level. *Nature Climate Change, 11*(6), 514-520. doi: 10.1038/s41558-021-01046-1

Dangendorf, S., Hay, C., Calafat, F. M., Marcos, M., Piecuch, C. G., Berk, K., et al. (2019), Persistent acceleration in global sea-level rise since the 1960s. *Nature Climate Change, 9*(9), 705-710. doi: 10.1038/s41558-019-0531-8

Duan, J., Li, Y., Wang, F., Hu, A., Han, W., Zhang, L., et al. (2021), Rapid sea-level rise in the Southern-Hemisphere subtropical oceans. *Journal of Climate, 34*(23), 9401-9423. doi: 10.1175/JCLI-D-21-0248.1

Fasullo, J. T., & Nerem, R. S. (2018), Altimeter-era emergence of the patterns of forced sea-level rise in climate models and implications for the future. *Proceedings of the National Academy of Sciences, 115*(51), 12944–12949. doi: 10.1073/pnas.1813233115

Feng, M., Li, Y., & Meyers, G. (2004), Multidecadal variations of Fremantle sea level: Footprint of climate variability in the tropical Pacific. *Geophysical Research Letters, 31* (16), L16302. doi: 10.1029/2004GL019947

Frederikse, T., Landerer, F., Caron, L., Adhikari, S., Parkes, D., Humphrey, V. W., et al. (2020), The causes of sea-level rise since 1900. *Nature, 584*(7821), 393–397. doi: 10.1038/s41586-020-2591-3

Fu, L.-L., & Qiu, B. (2002), Low-frequency variability of the north Pacific Ocean: The roles of boundary- and wind-driven baroclinic Rossby waves. *Journal of Geophysical Research: Oceans, 107*(C12), 3220. doi: 10.1029/2001JC001131

Hamlington, B. D., Leben, R. R., Strassburg, M. W., Nerem, R. S., & Kim, K.-Y. (2013), Contribution of the Pacific Decadal Oscillation to global mean sea level trends. *Geophysical Research Letters, 40*(19), 5171–5175. doi: 10.1002/grl.50950

Han, W., Stammer, D., Thompson, P., Ezer, T., Palanisamy, H., Zhang, X., et al. (2019), Impacts of basin-scale climate modes on coastal sea level: A review. *Surveys in Geophysics, 40*(6), 1493–1541. doi: 10.1007/s10712-019-09562-8

Henley, B. J., Gergis, J., Karoly, D. J., Power, S., Kennedy, J., & Folland, C. K. (2015), A Tripole Index for the Interdecadal Pacific Oscillation. *Climate Dynamics, 45*(11-12), 3077-3090. doi: 10.1007/s00382-015-2525-1

Holbrook, N. J., Goodwin, I. D., McGregor, S., Molina, E., & Power, S. B. (2011), ENSO to multi-decadal time scale changes in East Australian Current transports and Fort Denison sea level: Oceanic Rossby waves as the connecting mechanism. *Deep Sea Research Part II: Topical Studies in Oceanography, 58*(5), 547-558. doi: 10.1016/j.dsr2.2010.06.007

Huang, N. E., Shen, Z., Long, S. R., Wu, M. C., Shih, H. H., Zheng, Q., et al. (1998), The empirical mode decomposition and the Hilbert spectrum for nonlinear and non-stationary time series analysis. *Proceedings of the Royal Society of London. Series A: Mathematical, Physical and Engineering Sciences, 454*(1971), 903–995. doi: 10.1098/rspa.1998.0193

Huang, N. E., & Wu, Z. (2008), A review on Hilbert-Huang transform: Method and its applications to geophysical studies. *Reviews of Geophysics, 46*(2), RG2006. doi: 10.1029/2007RG000228

Ji, F., Wu, Z., Huang, J., & Chassignet, E. P. (2014), Evolution of land surface air temperature trend. *Nature Climate Change, 4*(6), 462–466. doi: 10.1038/nclimate2223

Kalnay, E., Kanamitsu, M., Kistler, R., Collins, W., Deaven, D., Gandin, L., et al. (1996), The NCEP/NCAR 40-year reanalysis project. B*ulletin of the American Meteorological Society, 77*(3), 437–471. doi: 10.1175/1520-0477(1996)077<0437:TNYRP>2.0.CO;2

Le Traon, P. Y., Nadal, F., & Ducet, N. (1998), An improved mapping method of multisatellite altimeter data. *Journal of Atmospheric and Oceanic Technology, 15*(2), 522-534. doi: 10.1175/1520-0426(1998)015<0522:AIMMOM>2.0.CO;2

Merrifield, M. A., & Maltrud, M. E. (2011), Regional sea level trends due to a Pacific trade wind intensification. *Geophysical Research Letters, 38*, L21605. doi: 10.1029/2011GL049576

Merrifield, M. A., Thompson, P. R., & Lander, M. (2012), Multidecadal sea

level anomalies and trends in the western tropical Pacific. *Geophysical Research Letters, 39*, L13602. doi: 10.1029/2012GL052032

Merrifield, M. A., & Thompson, P. R. (2018), Interdecadal sea level variations in the Pacific: Distinctions between the tropics and extratropics. *Geophysical Research Letters, 45*(13), 6604–6610. doi: 10.1029/2018GL077666

Munk, W. (2003), Ocean freshening, sea level rising. *Science, 300*(5628), 2041-2043. doi: 10.1126/science.1085534

Nerem, R. S., Chambers, D. P., Choe, C., & Mitchum, G. T. (2010), Estimating mean sea level change from the TOPEX and Jason altimeter missions. *Marine Geodesy, 33*(S1), 435–446. doi: 10.1080/01490419.2010.491031

Nerem, R. S., & G. T. Mitchum (2002), Estimates of vertical crustal motion derived from differences of TOPEX/POSEIDON and tide gauge sea level measurements. *Geophysical Research Letters, 29*(19), 1934. doi: 10.1029/2002GL015037

Qian, C. (2015), On trend estimation and significance testing for non-Gaussian and serially dependent data: Quantifying the urbanization effect on trends in hot extremes in the megacity of Shanghai. *Climate Dynamics, 47*(1-2), 329-344. doi: 10.1007/s00382-015-2838-0

Qiu, B., & Chen, S. (2006), Decadal variability in the large-scale sea surface height field of the South Pacific Ocean: Observations and causes. *Journal of Physical Oceanography, 36*(9), 1751-1762. doi: 10.1175/JPO2943.1

Qu, T., Fukumori, I., & Fine, R. A. (2019), Spin-up of the Southern Hemisphere super gyre. *Journal of Geophysical Research: Oceans, 124*(1), 154–170. doi: 10.1029/2018JC014391

Roemmich, D., Gilson, J., Davis, R., Sutton, P., Wijffels, S., & Riser, S. (2007), Decadal spinup of the South Pacific subtropical gyre. *Journal of Physical Oceanography, 37*(2), 162-173. doi: 10.1175/JPO3004.1

Sasaki, Y. N., Minobe, S., Schneider, N., Kagimoto, T., Nonaka, M., & Sasaki, H. (2008), Decadal sea level variability in the South Pacific in a global eddy-resolving ocean model hindcast. *Journal of Physical Oceanography, 38*(8), 1731-1747. doi: 10.1175/2007JPO3915.1

Schneider, N., Miller, A. J., & Pierce, D. W. (2002), Anatomy of North Pacific decadal variability. *Journal of Climate, 15*(6), 586-605. doi: 10.1175/1520-0442(2002)015<0586:AONPDV>2.0.CO;2

Stocker, T. F., Qin, D., Plattner, G.-K., Tignor, M., Allen, S. K., Boschung, J., et al. (Eds.) (2013), Intergovernmental Panel on Climate Change (2013). Climate Change 2013: The Physical Science Basis. Contribution of Working Group I to the Fifth Assessment Report of the Intergovernmental Panel on Climate Change. Cambridge Univ. Press, Cambridge, U. K., and New York.

Thompson, D. W. J., Wallace, J. M., & Hegerl, G. C. (2000), Annular modes in the extratropical circulation. Part II: Trends. *Journal of Climate, 13*(5),

1018-1036. doi: 10.1175/1520-0442(2000)013<1018:AMITEC>2.0.CO;2

Woodworth, P. L., & Player, R. (2003), The permanent service for mean sea level: An update to the 21st century. *Journal of Coastal Research, 19*(2), 287–295. doi: 10.2112/JCOASTRES-D-12-00

Wu, Z., & Huang, N. E. (2009), Ensemble empirical mode decomposition: A noise-assisted data analysis method. *Advances in Adaptive Data Analysis, 1*(1), 1-41. doi: 10.1142/S1793536909000047

Zhang, L., & Qu, T. (2015), Low-frequency variability of the South Pacific subtropical gyre as seen from satellite altimetry and Argo. *Journal of Physical Oceanography, 45*(12), 3083-3098. doi: 10.1175/JPO-D-15-0026.1